H1prelim-18-071, ZEUS-prel-17-01-extension
February 22, 2018

Combination and QCD analysis of beauty and charm production cross section measurements in deep inelastic ep scattering at HERA

The H1 and ZEUS Collaborations

Abstract

Measurements of open charm and beauty production cross sections in deep inelastic ep scattering at HERA from the H1 and ZEUS Collaborations are combined. Reduced cross sections are obtained in the kinematic range of negative four-momentum transfer squared of the photon $2.5\ \text{GeV}^2 \leq Q^2 \leq 2000\ \text{GeV}^2$ and Bjorken scaling variable $3 \cdot 10^{-5} \leq x_{\text{Bj}} \leq 5 \cdot 10^{-2}$. The combination method accounts for the correlations of the statistical and systematic uncertainties among the different data sets. Perturbative QCD calculations are compared to the combined data. A next-to-leading order QCD analysis is performed using these data together with the combined inclusive deep inelastic scattering cross sections from HERA. This document contains additional figures for the preliminary results given in H1prelim-17-071/ZEUS-prel-17-01.

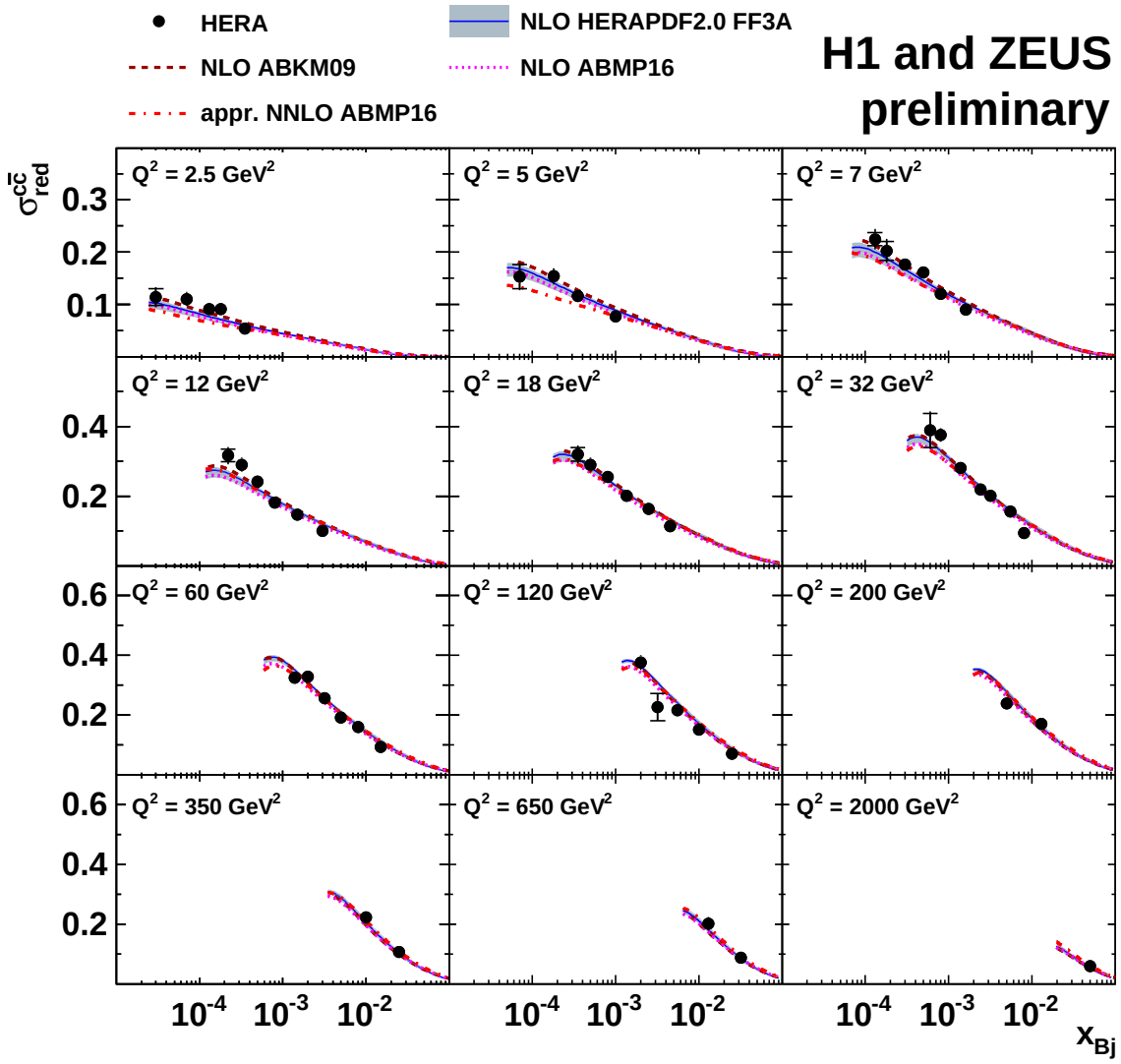

Figure 1: Combined reduced charm cross sections, $\sigma^{c\bar{c}}_{\mathrm{red}}$, (full circles) as a function of x_{Bj} for given values of Q^2, compared to the NLO QCD FFNS predictions based on the HERAPDF2.0 FF3A (solid lines), ABKM09 (dashed lines) and ABMP16 (dotted lines) PDF sets. Also shown is the approximate NNLO prediction using ABMP16 (dashed-dotted lines). The shaded bands on the HERAPDF2.0 FF3A predictions show the theory uncertainties obtained by adding PDF, scale and charm quark mass uncertainties in quadrature.

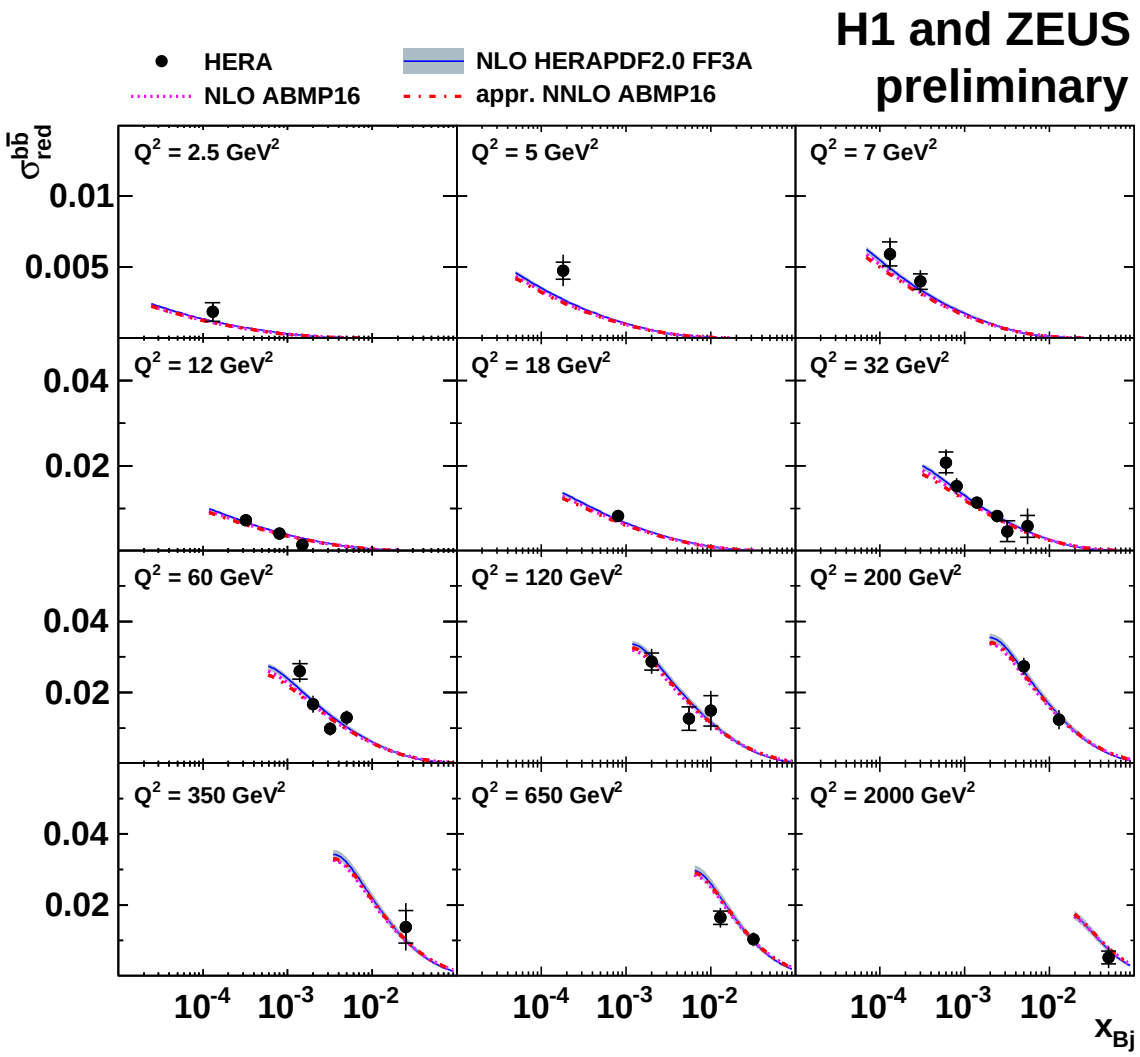

Figure 2: Combined reduced beauty cross sections, $\sigma^{b\bar{b}}_{\mathrm{red}}$, (full circles) as a function of x_{Bj} for given values of Q^2, compared to the NLO QCD FFNS predictions based on the HERAPDF2.0 FF3A (solid lines), ABKM09 (dashed lines) and ABMP16 (dotted lines) PDF sets. Also shown is the prediction in approximate NNLO using ABMP16 (dashed-dotted lines). The shaded bands on the HERAPDF2.0 FF3A predictions show the theory uncertainties obtained by adding PDF, scale and beauty quark mass uncertainties in quadrature.

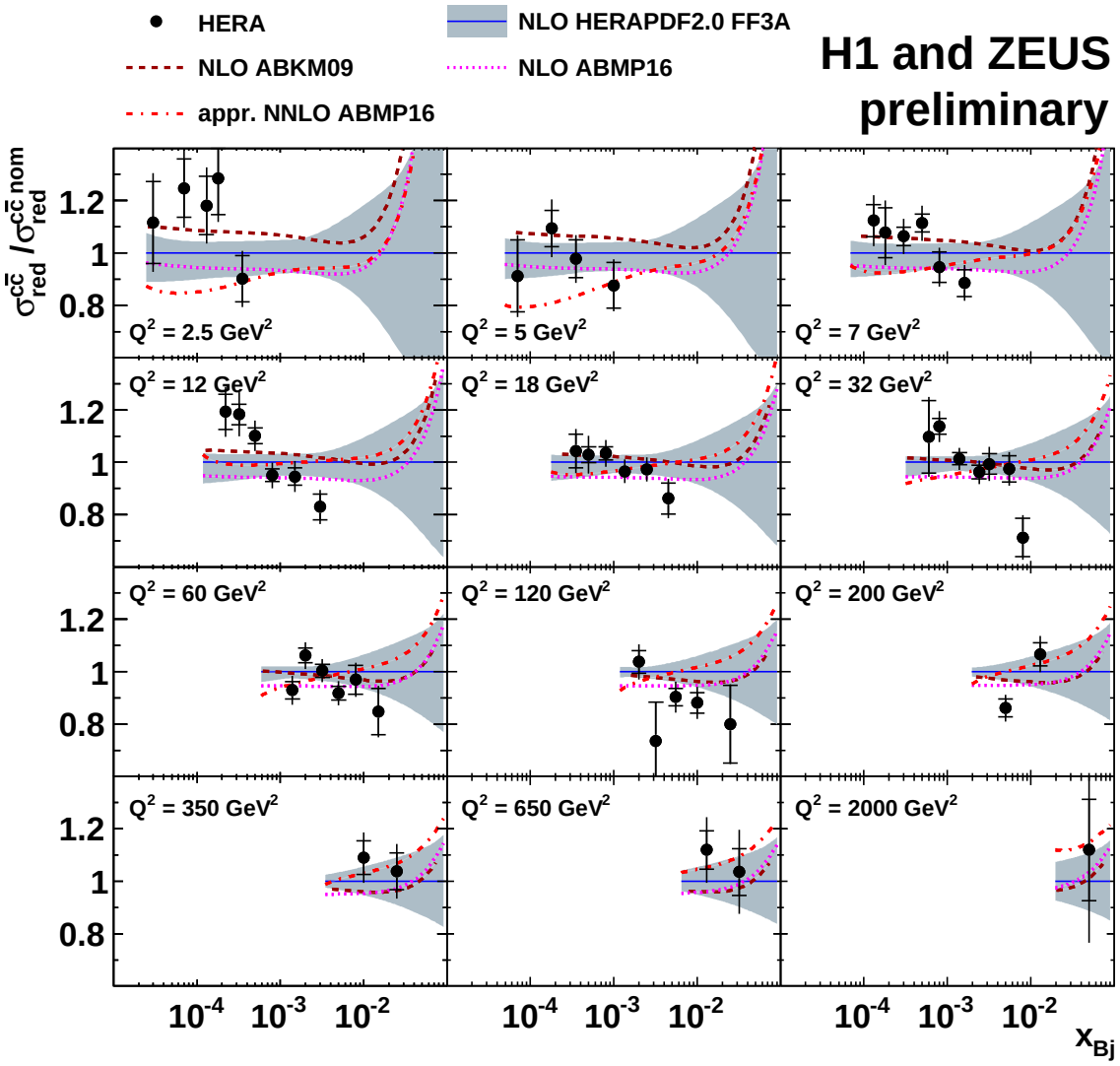

Figure 3: Combined reduced charm cross sections, $\sigma_{\mathrm{red}}^{c\bar{c}}$, (full circles) as a function of x_{Bj} for given values of Q^2, compared to the NLO (dashed and dotted lines) and approximate NNLO (dashed-dotted lines) QCD theoretical FFNS predictions obtained using various PDFs, as in Fig. 1, normalised to the predictions obtained using HERAPDF2.0 FF3A (solid lines with shaded uncertainty bands).

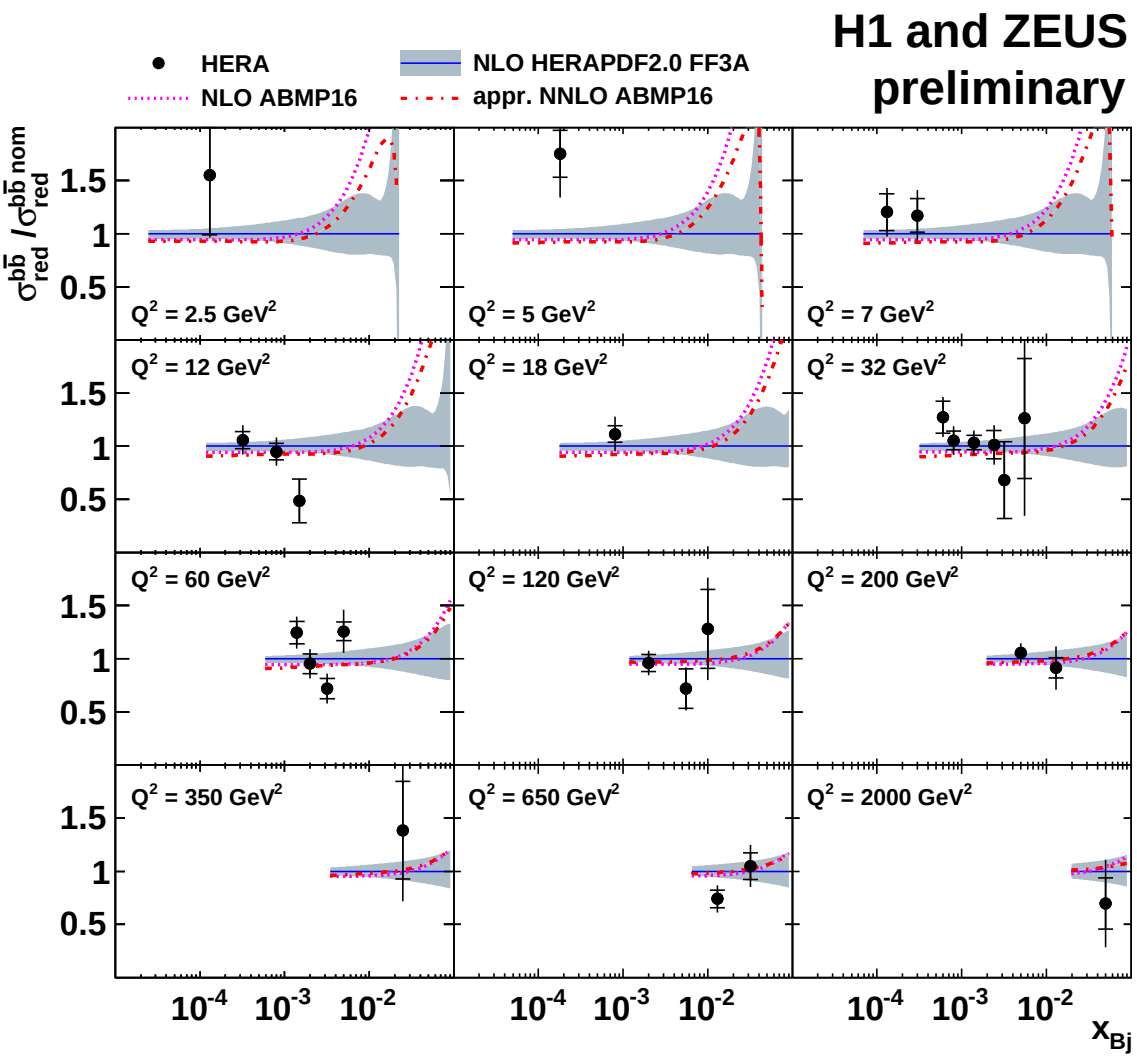

Figure 4: Combined reduced beauty cross sections, $\sigma_{\mathrm{red}}^{b\bar{b}}$, (full circles) as a function of x_{Bj} for given values of Q^2, compared to the NLO (dotted bands) and approximate NNLO (dashed-dotted bands) QCD theoretical FFNS predictions obtained using various PDFs, as in Fig. 2, normalised to the predictions obtained using HERAPDF2.0 FF3A (solid lines with shaded uncertainty bands).

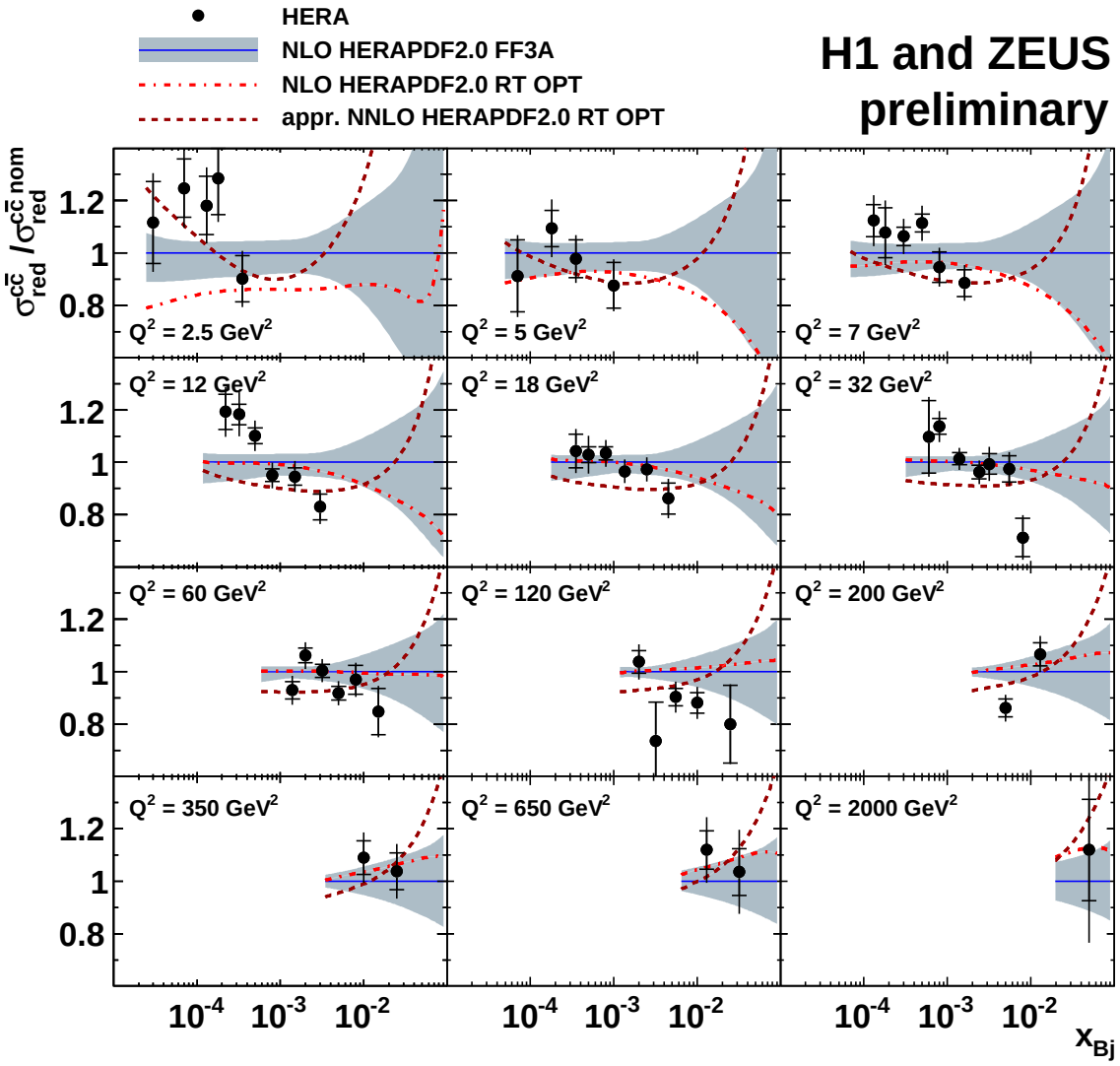

Figure 5: Combined reduced charm cross sections, $\sigma_{\mathrm{red}}^{c\bar{c}}$, (full circles) as a function of x_{Bj} for given values of Q^2, compared to NLO (dashed-dotted lines) and approximate NNLO (dashed lines) VFNS predictions based on HERAPDF2.0 using corresponding NLO and NNLO HERAPDF2.0 PDF sets, normalised to the FFNS predictions obtained using HERAPDF2.0 FF3A (solid lines with shaded uncertainty bands). The uncertainties for the VFNS predictions are of similar size to those presented for the FFNS calculation.

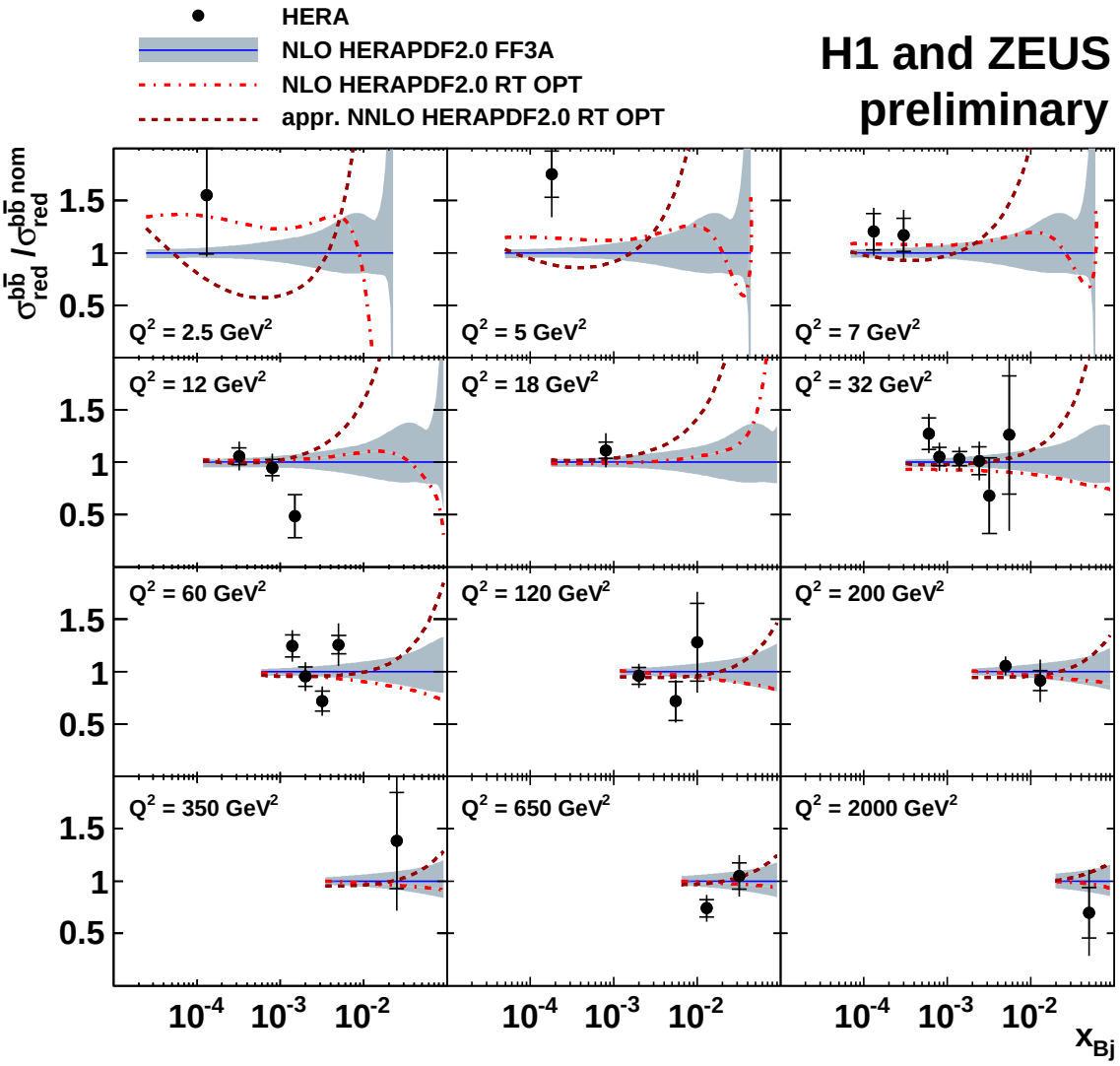

Figure 6: Combined reduced beauty cross sections, $\sigma_{\mathrm{red}}^{b\bar{b}}$, (full circles) as a function of x_{Bj} for given values of Q^2, compared to the NLO (dashed-dotted lines) and approximate NNLO (dashed lines) VFNS predictions based on HERAPDF2.0 using corresponding NLO and NNLO HERAPDF2.0 PDF sets, normalised to the FFNS predictions obtained using HERAPDF2.0 FF3A (solid lines with shaded uncertainty bands). For the VFNS predictions no uncertainties are given. These are in size similar to those presented for the FFNS calculation.

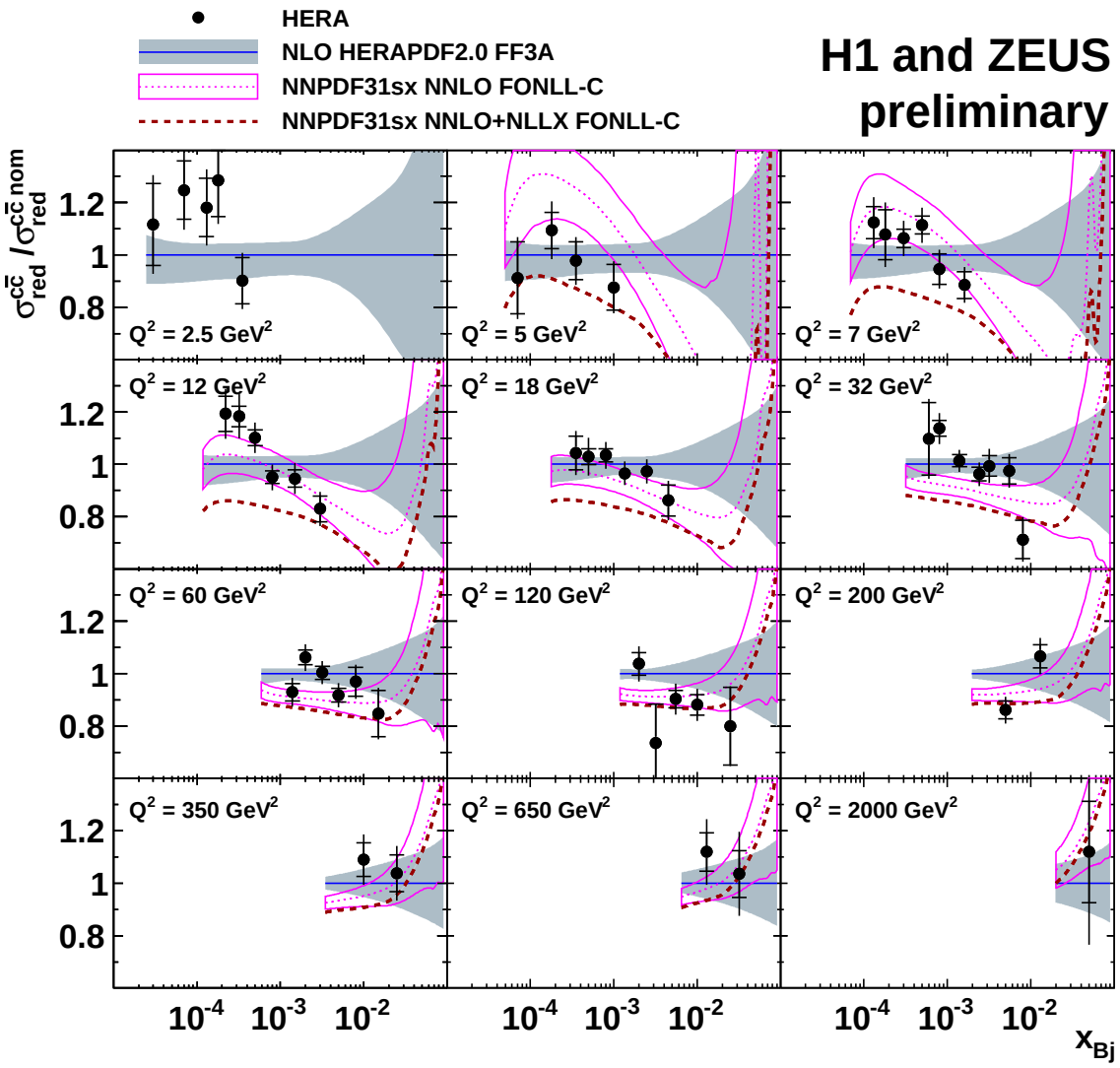

Figure 7: Combined reduced charm cross sections, $\sigma_{\mathrm{red}}^{c\bar{c}}$, (full circles) as a function of x_{Bj} for given values of Q^2, compared to VFNS predictions of the NNPDF group normalised to the FFNS predictions obtained using HERAPDF2.0 FF3A (solid lines with shaded uncertainty bands). Results from two different calculations are shown: without (FONNL-C, dotted lines with uncertainty bands) and with low-x resummation (FONNL-C+NLLsx , dashed lines). For the calculations the NNPDF3.1sx PDF set is used. For better clarity of the presentation the uncertainties of the FONNL+NLLsx calculations are not shown. These are in size similar to those shown for the FONLL calculations. No FONNL predictions based on NNPDF3.1sx are shown at $Q^2 = 2.5$ GeV^2 because this value lies below the starting scale of the QCD evolution in the calculation (2.6 GeV^2).

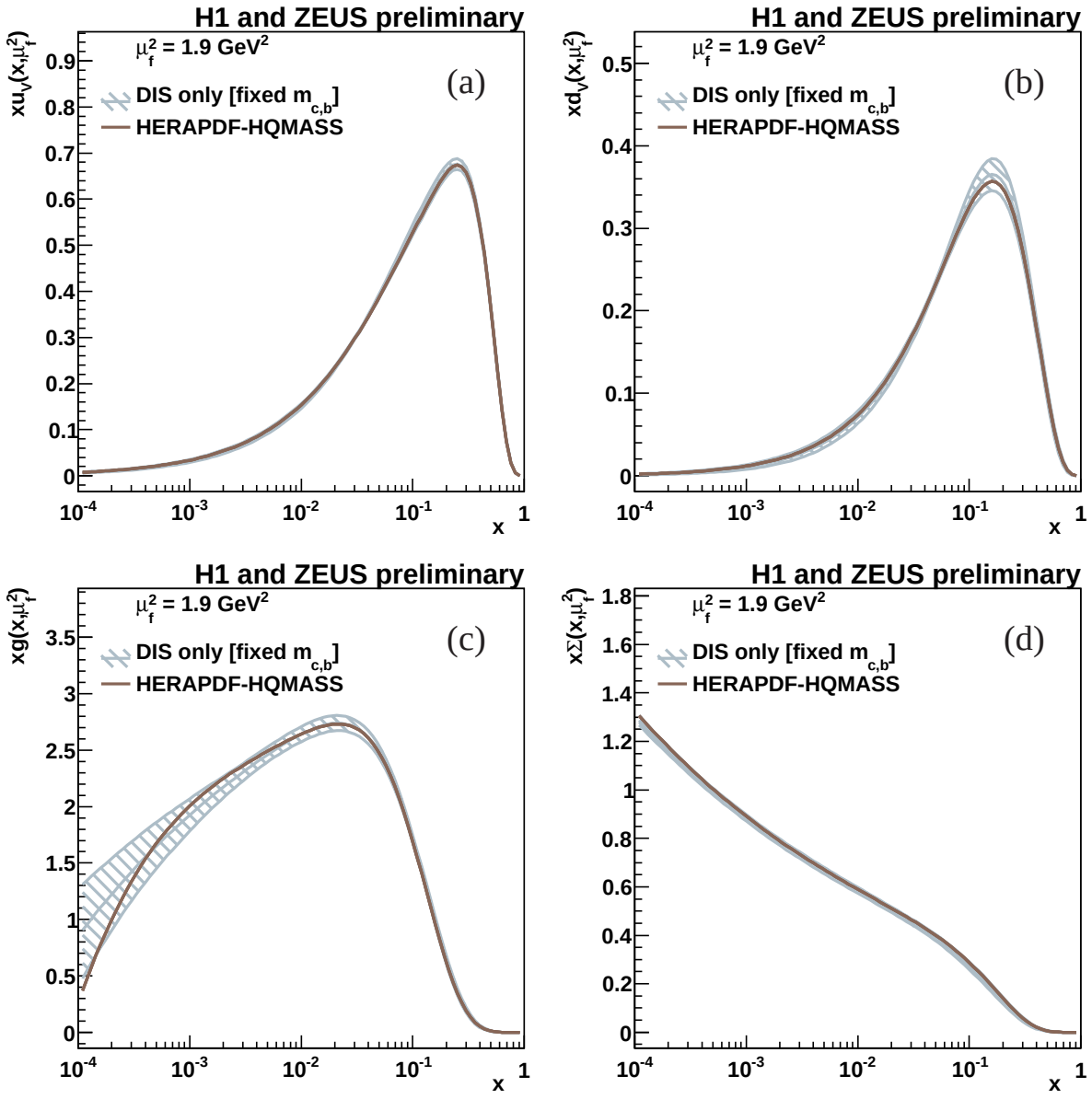

Figure 8: Parton density functions $x \cdot f(x, Q^2)$ at the starting scale $Q_0^2 = 1.9$ GeV^2 with $f = u_v, d_v, g, \Sigma$ for the valence up quark (a), the valence down quark (b), the gluon (c) and the sea quarks (d) of the resulting PDF set, termed HERAPDF-HQMASS (solid dark lines), and obtained from a fit to the combined inclusive data only (light grey lines). The experimental/fit uncertainties obtained from the fit to the combined inclusive and heavy flavour data are indicated by the hatched bands. For better visibility only the uncertainties for the fit to the inclusive data are shown.

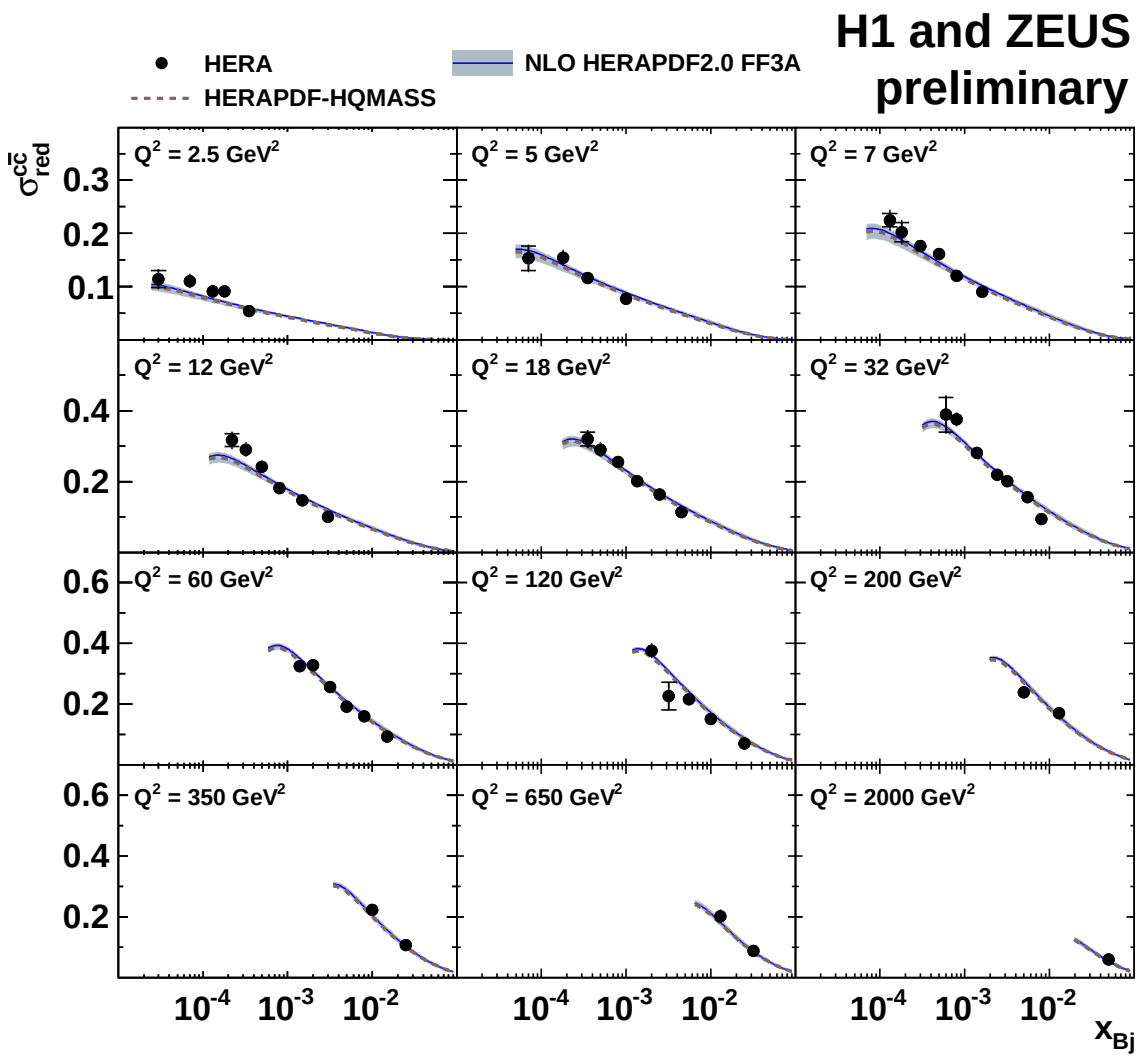

Figure 9: Combined reduced charm cross sections, $\sigma_{\mathrm{red}}^{c\bar{c}}$, (full circles) as a function of x_{Bj} for given values of Q^2, compared to the NLO QCD FFNS predictions based on HERAPDF-HQMASS (dashed lines) and on HERAPDF2.0 FF3A (solid lines). The shaded bands on the HERAPDF2.0 FF3A predictions show the theory uncertainties obtained by adding PDF, scale and charm quark mass uncertainties in quadrature.

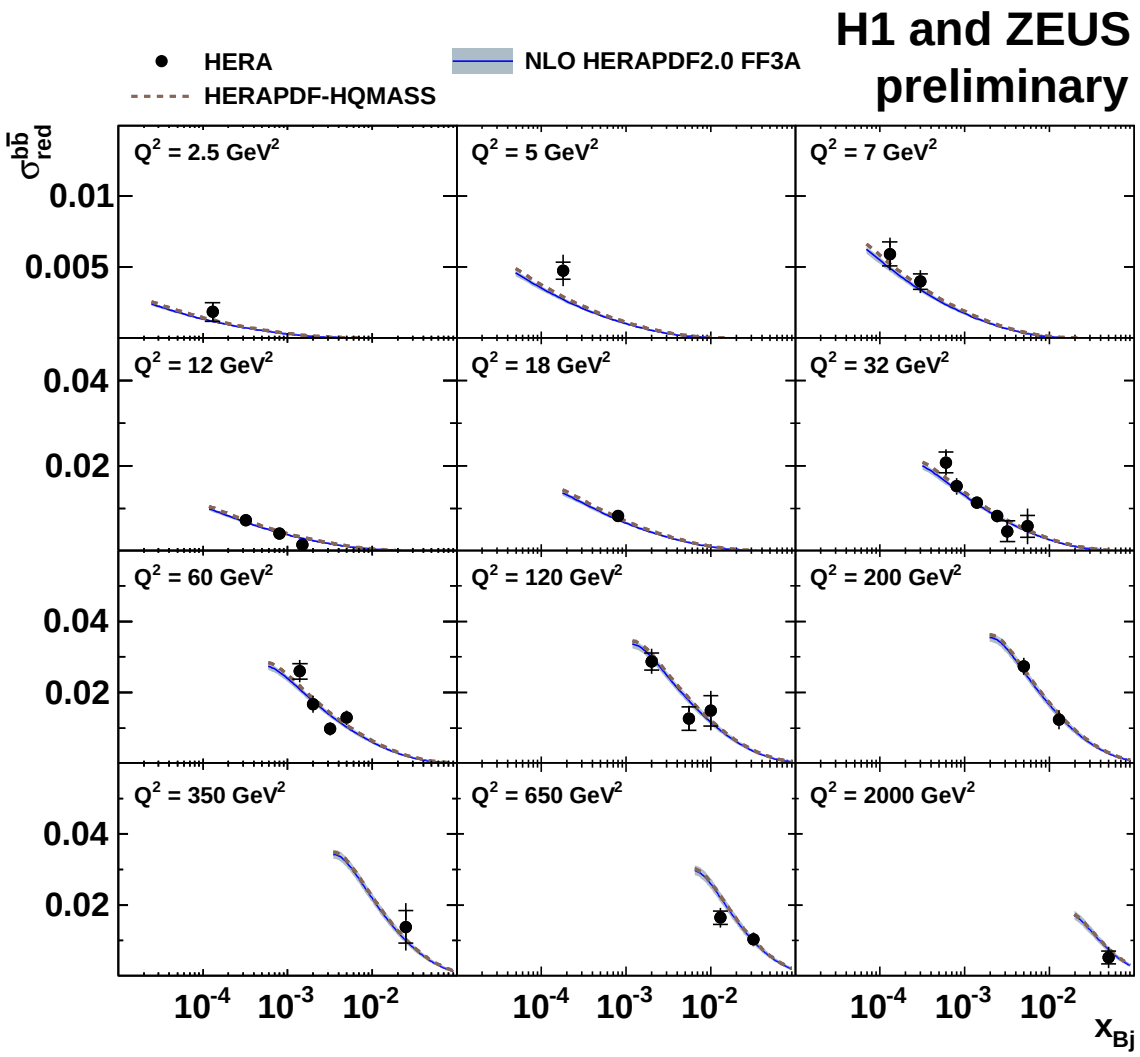

Figure 10: Combined reduced beauty cross sections, $\sigma^{b\bar{b}}_{\mathrm{red}}$, (full circles) as a function of x_{Bj} for given values of Q^2, compared to the NLO QCD FFNS predictions based on HERAPDF-HQMASS (dashed lines) and on HERAPDF2.0 FF3A (solid lines). The shaded bands on the predictions using the fitted PDF set show the theory uncertainties obtained by adding PDF, scale and charm quark mass uncertainties in quadrature.

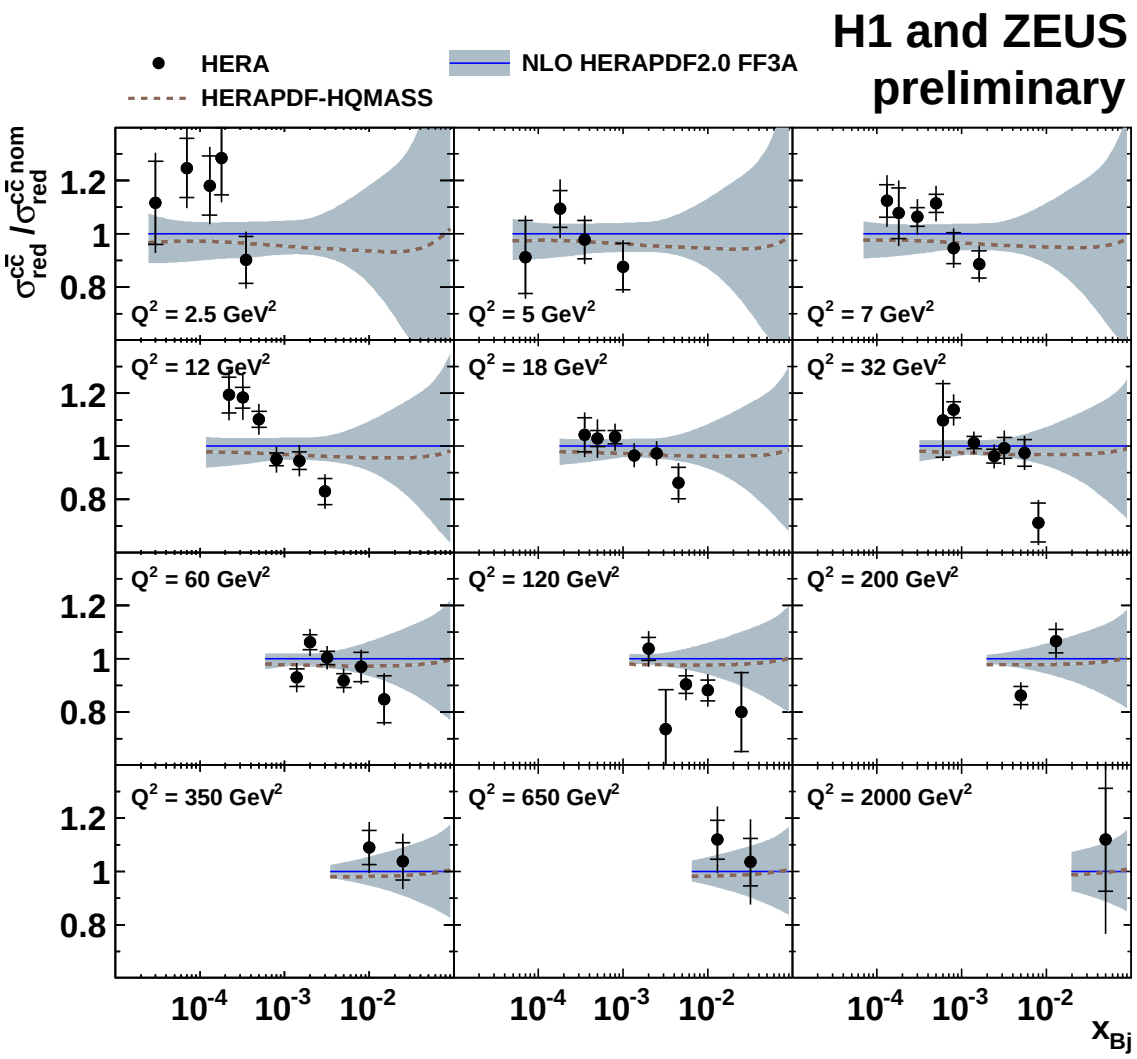

Figure 11: Combined reduced charm cross sections, $\sigma_{red}^{c\bar{c}}$, (full circles) as a function of x_{Bj} for given values of Q^2, compared to the NLO FFNS predictions using HERAPDF-HQMASS (dashed lines), normalised to the reference cross sections using HERAPDF2.0 FF3A (solid lines with uncertainty bands).

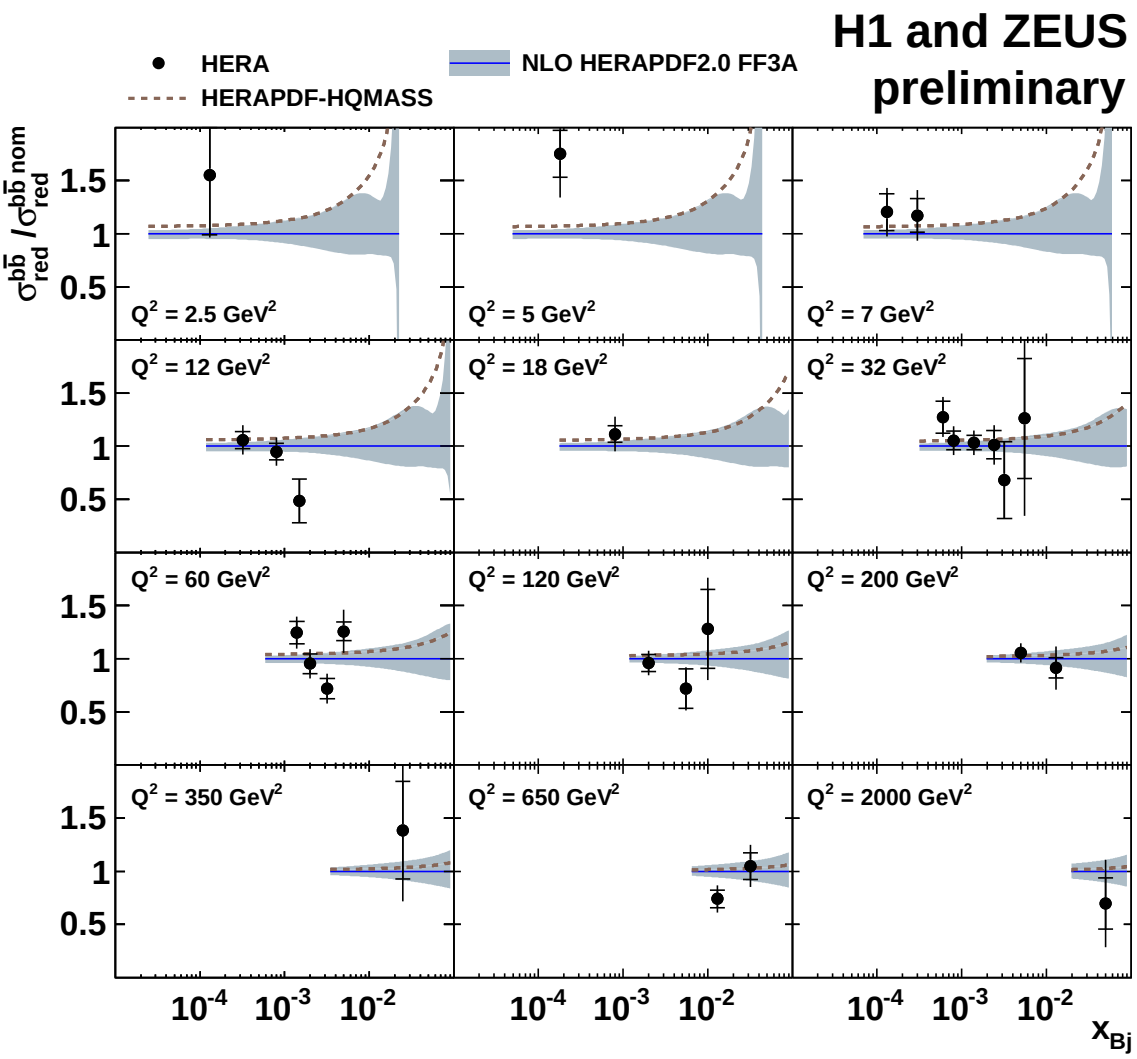

Figure 12: Combined reduced beauty cross sections, $\sigma_{\mathrm{red}}^{b\bar{b}}$, (full circles) as a function of x_{Bj} for given values of Q^2, compared to the NLO FFNS predictions using HERAPDF-HQMASS (dashed lines), normalised to the reference cross sections using HERAPDF2.0 FF3A (solid lines with uncertainty bands).

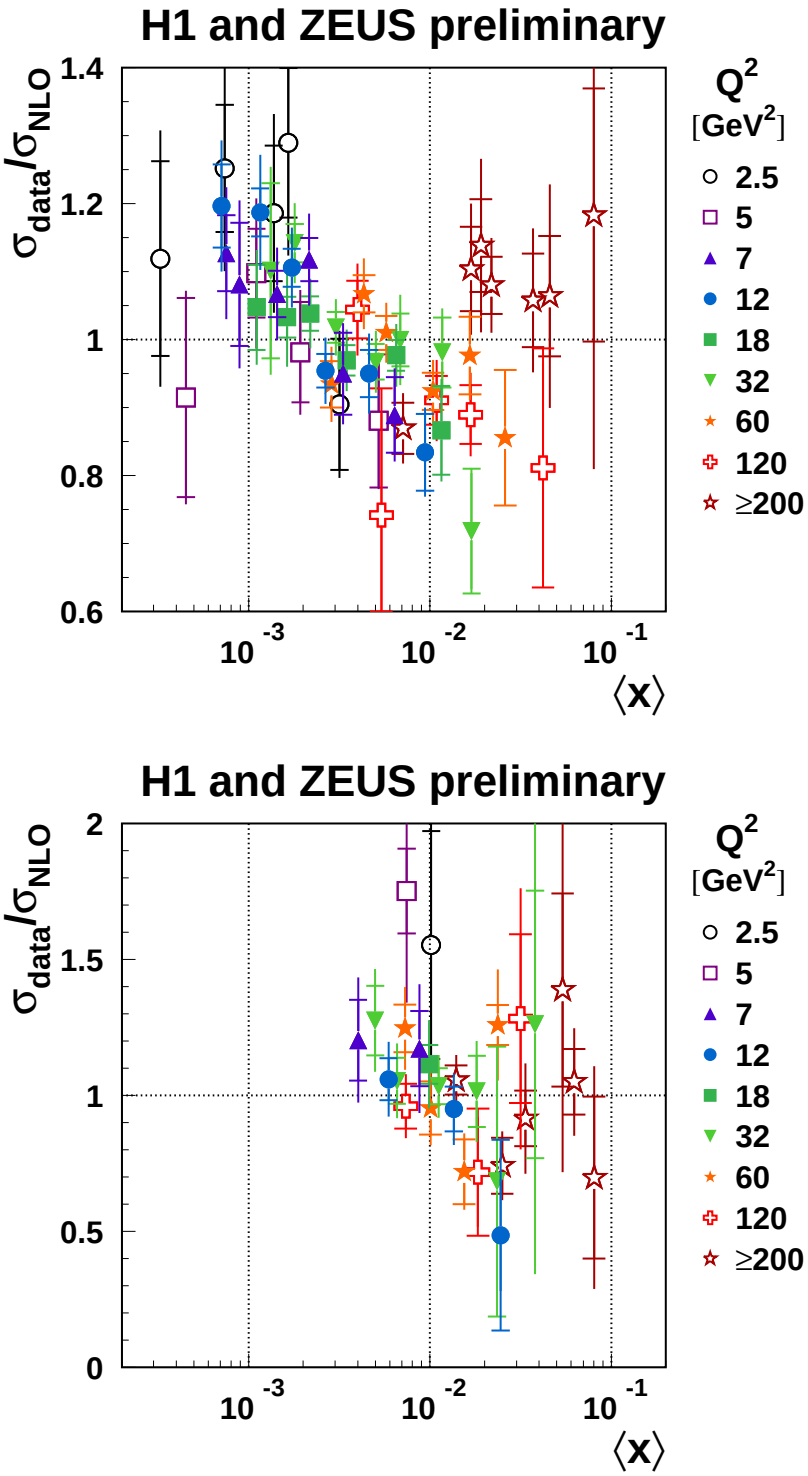

Figure 13: Ratio of the combined reduced cross sections, $\sigma_{\mathrm{red}}^{c\bar{c}}$ (a) and $\sigma_{\mathrm{red}}^{b\bar{b}}$ (b), to the NLO FFNS cross section predictions, based on HERAPDF-HQMASS, as a function of the partonic $\langle x \rangle$ for different values of Q^2.

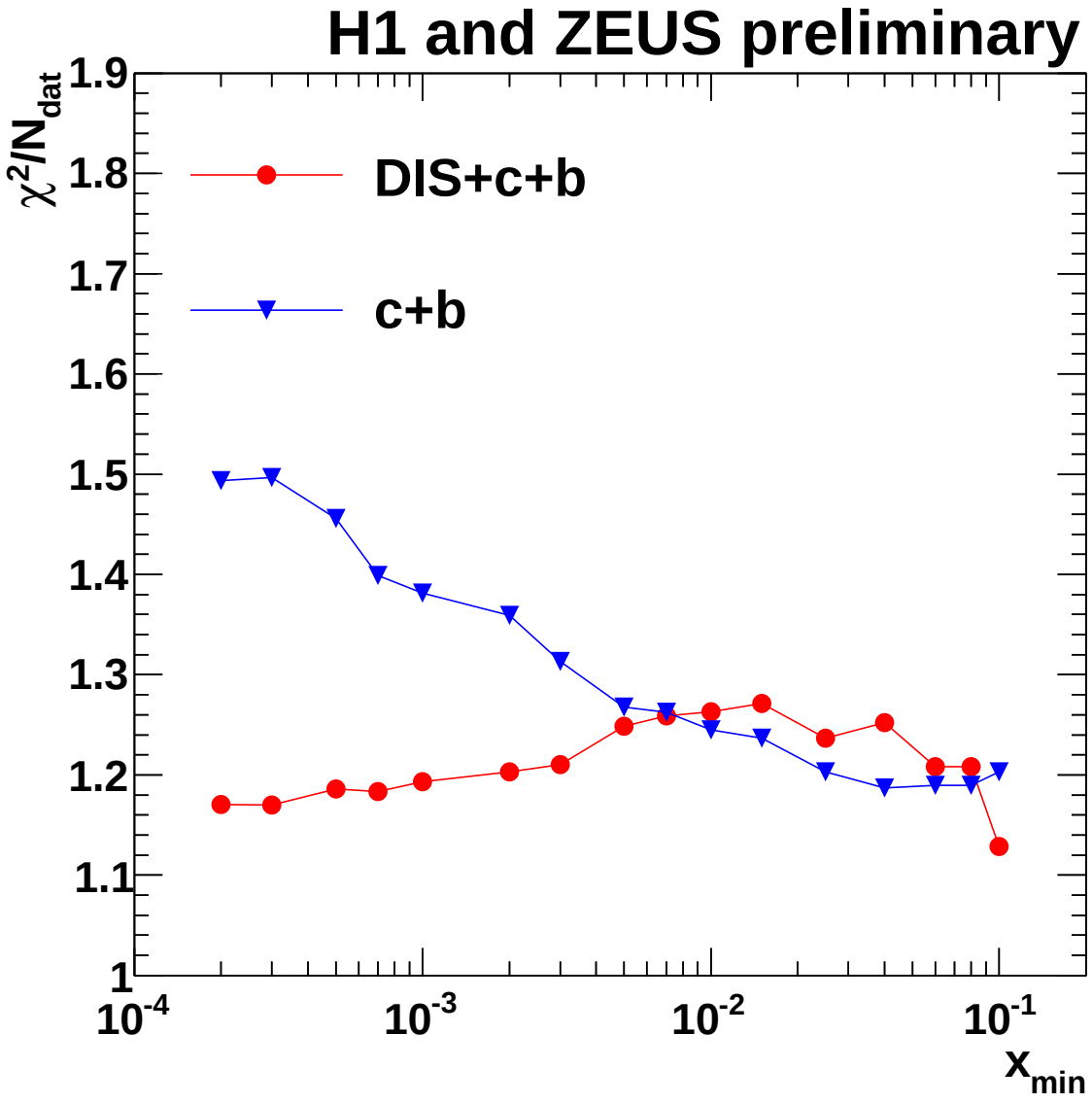

Figure 14: The values of χ^2 divided by the number of data point (N_{dat}) of the QCD fit to the inclusive and heavy flavour data: (triangles) for the heavy flavour data only and (dots) for the inclusive plus heavy flavour data when including in the fit only inclusive data with $x_{Bj} \geq x_{min}$.

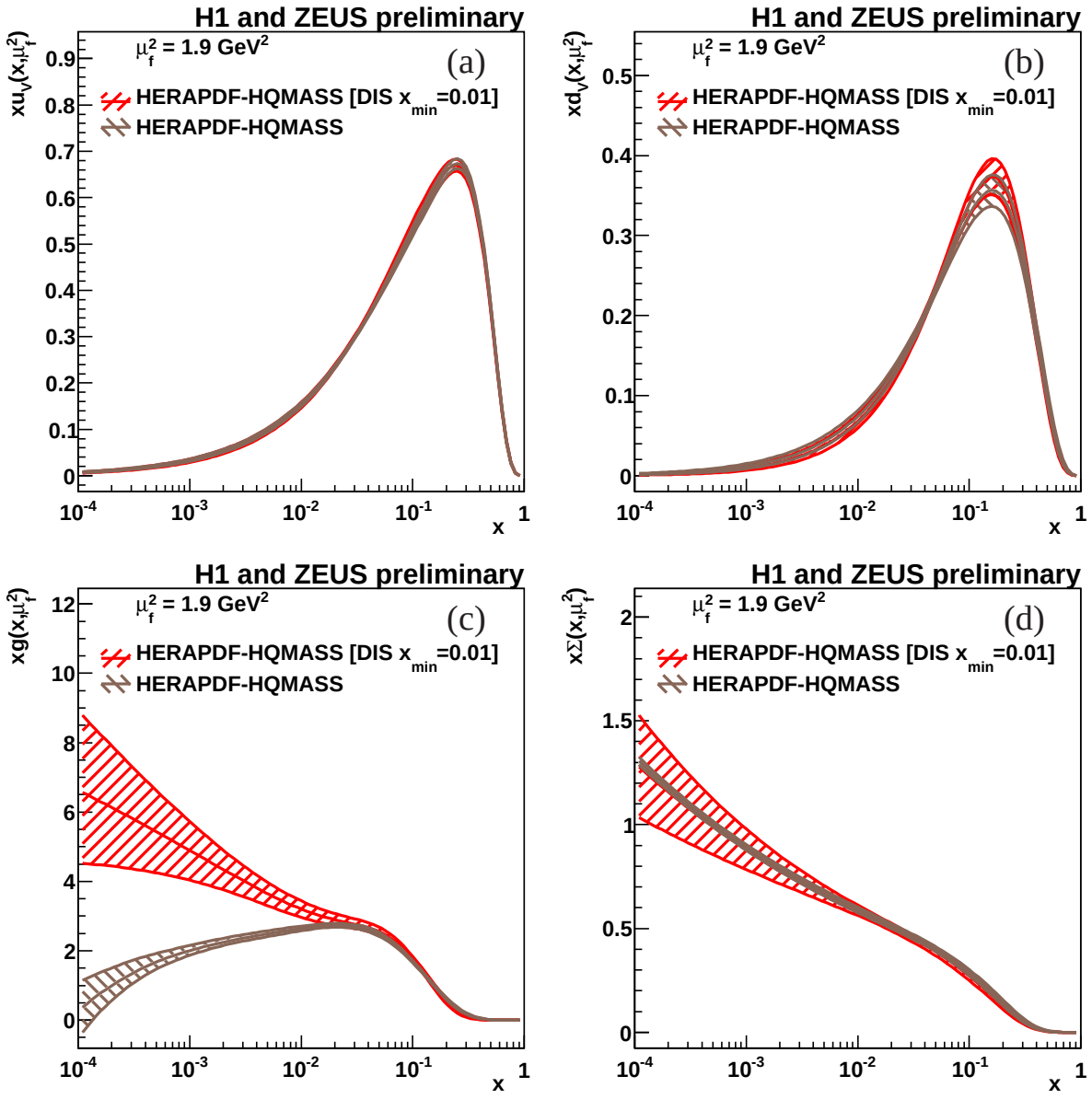

Figure 15: Parton density functions $x \cdot f(x, Q^2)$ at the starting scale $Q_0^2 = 1.9$ GeV^2 with $f = u_v, d_v, g, \Sigma$ for the valence up quark (a), the valence down quark (b), the gluon (c) and the sea quarks (d) of HERAPDF-HQMASS (full lines) and obtained from the QCD fit to the combined inclusive and heavy flavour data with imposing a minimum cut of $x_{\mathrm{Bj}} \geq 0.01$ to the inclusive data included in the fit. The experimental/fit uncertainties are shown by the hatched bands.

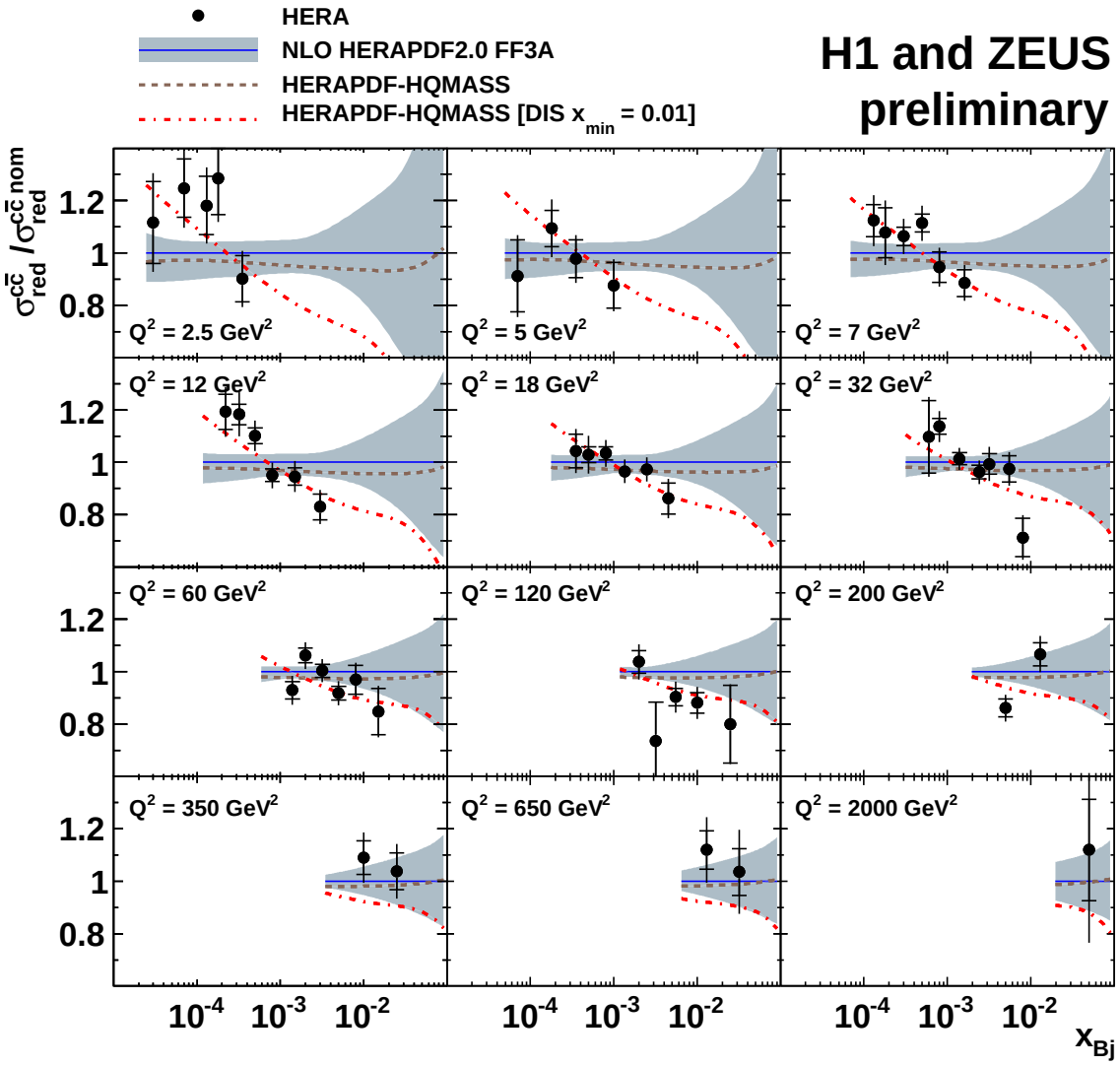

Figure 16: Combined reduced charm cross sections, $\sigma_{\mathrm{red}}^{c\bar{c}}$, (full circles) as a function of x_{Bj} for given values of Q^2, compared to the NLO FFNS predictions based on HERAPDF-HQMASS (dashed lines) and those resulting from the alternative fit when requiring $x_{\mathrm{Bj}} \geq 0.01$ for the inclusive data (dashed dotted lines, normalised to the reference cross sections using HERAPDF2.0 FF3A (full line). The experimental/fit uncertainties of the reference cross sections are indicated by the shaded bands.

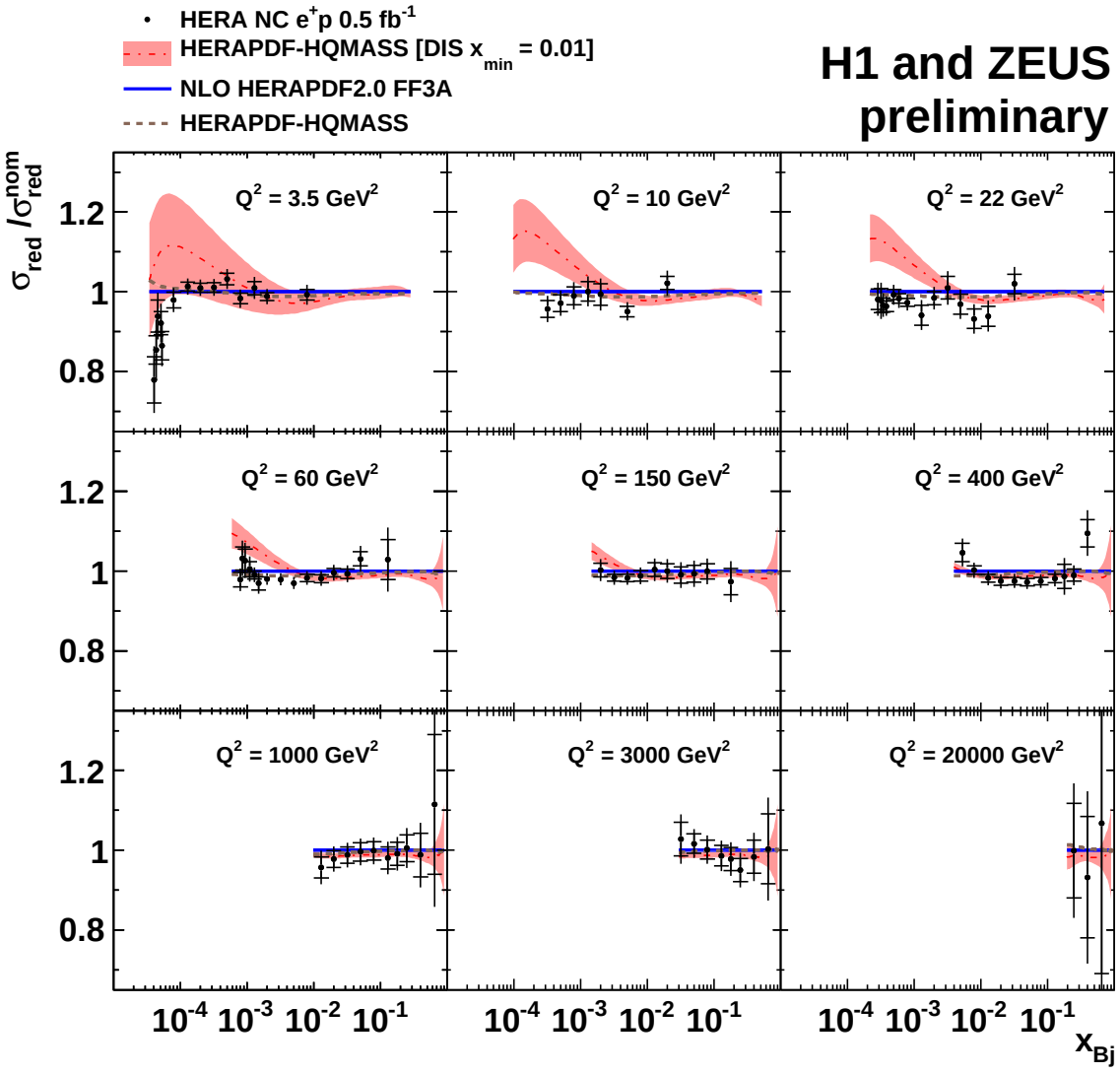

Figure 17: Combined reduced NC cross sections, σ_{red}, (full circles) as a function of x_{Bj} for selected values of Q^2, compared to the NLO FFNS predictions based on HERAPDF-HQMASS (dashed lines) and those resulting from the alternative fit with $x_{Bj} \geq 0.01$ required for the inclusive data (dashed-dotted lines), normalised to the reference cross sections using HERAPDF2.0 FF3A (solid lines).